Energy Conversion and Management 52 (2011) 1968–1973

Contents lists available at ScienceDirect

Energy Conversion and Management

journal homepage: www.elsevier.com/locate/enconman

On the heat transfer correlation for membrane distillation

Chi-Chuan Wang *

Department of Mechanical Engineering, National Chiao Tung University, Hsinchu 300, Taiwan

ARTICLE INFO

Article history:
Received 17 June 2009
Received in revised form 5 March 2010
Accepted 21 November 2010
Available online 8 January 2011

Keywords:
Membrane distillation
Heat transfer coefficient
Wilson plot

ABSTRACT

The present study examines the heat transfer coefficients applicable for membrane distillation. In the available literatures, researchers often adopt some existing correlations and claim the suitability of these correlations to their test data or models. Unfortunately this approach is quite limited and questionable. This is subject to the influences of boundary conditions, geometrical configurations, entry flow conditions, as well as some influences from spacer or support. The simple way is to obtain the heat transfer coefficients from experimentation. However there is no direct experimental data for heat transfer coefficients being reported directly from the measurements. The main reasons are from the uncertainty of permeate side and of the comparatively large magnitude of membrane resistance. Additional minor influence is the effect of mass transfer on the heat transfer performance. In practice, the mass transfer effect is negligible provided the feed side temperature is low. To increase the accuracy of the measured feed side heat transfer coefficient, it is proposed in this study to exploit a modified Wilson plot technique. Through this approach, one can eliminate the uncertainty from permeate side and reduce the uncertainty in membrane to obtain a more reliable heat transfer coefficients at feed side from the experimentation.

1. Introduction

Membrane distillation (MD) is a hybrid of thermal distillation and membrane processes. It features a thermally driven process via a microporous membrane separating the warm and cold solution. The vapor pressure difference is generated through the non isothermal process amid feed side and permeate side, thereby vapor molecules will transport through from the warm feed side into the hydrophobic membrane pores provided the vapor pressure is being established. Fig. 1 is a schematic showing the typical MD membrane and its heat/mass transport mechanisms. Evaporation occurs at the warm feed side, yet the vapor molecules migrate across the non wetted pores to condense at the permeate side. The overall heat transfer process is described subsequently.

From this schematic, heat is first transferred from the warm solution across the thermal boundary layer:

$$q_f = h_f(T_f - T_{m1}) \tag{1}$$

Here q_f is the convective heat transfer flux and h_f is the heat transfer coefficient at the feed side. The heat transfer within the membrane (q_m) is divided in parallel into conduction across the membrane material (q_c) as well as the heat subject to vapor flowing through the membrane (q_v), yet the relevant heat transfer equation inside the membrane is given by [1]:

$$q_m = J\lambda + \frac{k_m}{\delta}(T_{m1} - T_{m2}) \tag{2}$$

where J is the evaporative mass flux across the membrane and λ is the heat of vaporation. The effective thermal conductivity of the membrane can be determined as the following

$$k_m = (1-\varepsilon)k_s + \varepsilon k_g \tag{3}$$

where ε denotes porosity of the membrane material, and k_s and k_g are the thermal conductivity for solid (polymer) and gas in the pore.

Analogously, the heat transfer from the membrane to the permeate side is given by:

$$q_p = h_p(T_{m2} - T_p) \tag{4}$$

At steady state conditions, the heat flux is expressed by:

$$q = q_f = q_m = q_p \tag{5}$$

Rearranging Eqs. (1)–(4) yield

$$q = \frac{T_f - T_p}{\left(\frac{1}{h_f} + \frac{1}{\frac{k_m}{\delta} + \frac{J\lambda}{\Delta T_m}} + \frac{1}{h_p}\right)} \tag{6}$$

As clearly seen from Eq. (6), three resistances prevails for the heat transport from warm feed side to cold permeate side, namely the convective resistance of feed side ($1/h_f$) and permeate side ($1/h_p$) and the membrane resistance $\left(\frac{1}{\frac{k_m}{\delta} + \frac{J\lambda}{\Delta T_m}}\right)$. Normally the feed side

* Address: EE474, 1001 University Road, Hsinchu 300, Taiwan. Tel.: +886 3 5712121x55105; fax: +886 3 5820634.
E-mail address: ccwang@mail.nctu.edu.tw

0196-8904/$ - see front matter © 2010 Elsevier Ltd. All rights reserved.
doi:10.1016/j.enconman.2010.11.014

Nomenclature

A	surface area (m^2)
c_p	specific heat (kJ/kg K)
D	diameter (m)
h	heat transfer coefficient (W/m^2 K)
J	evaporative flux (kg/m^2 s)
k	thermal conductivity (W/m K)
$\dot{m}$	mass flow rate (kg/s)
Nu	Nusselt number
Pr	Prandtl number
q	heat flux (W/m^2)
$\dot{Q}$	heat transfer rate (W)
R	resistance (m^2 K/W)
T	temperature (°C)
U	overall heat transfer coefficient (W/m^2 K)
v	velocity (m/s)

Greek symbols

ε	porosity
δ	membrane thickness (m)
ΔT_{LM}	log mean temperature difference (K)
ΔT_m	temperature difference across membrane (K)
λ	heat of evaporation (kJ/kg)
μ	dynamic viscosity (kg/m s)
ρ	density (kg/m^3)

Subscripts

ave	average value
f	feed side
g	gas phase
in	inlet
m	membrane
$m1$	membrane in contact with the feed side
$m2$	membrane in contact with the permeate side
out	outlet
p	permeate side
s	solid phase
t	total

resistance is larger than that of permeate side, yet it plays a crucial role in overall heat transport process of MD.

Of the literatures concerning with the heat transfer coefficients applicable to the feed side or permeate side, none of the existing literatures were really dealt with the data reduction of the collected data. Even for those researchers who perform substantial experiments in MD, there were no direct thermal resistances reported from their measurements. In fact, all the research works,

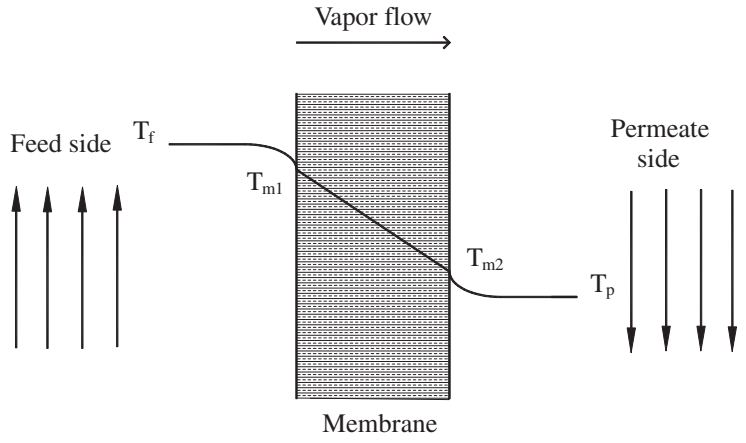

(a) Temperature variation for MD Process

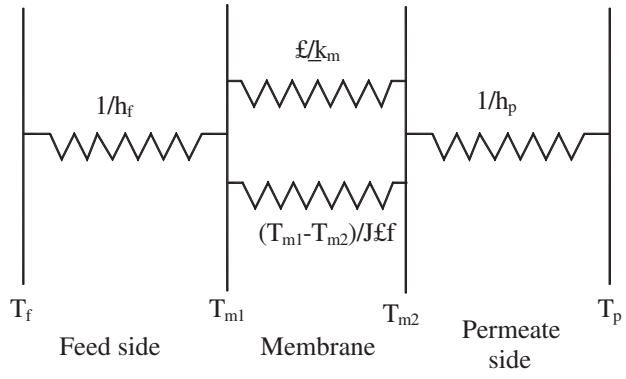

(b) Thermal Resistance Network

Fig. 1. Schematic showing the temperature variation for membrane distillation across and the associated thermal resistance network. (a) Temperature variation for MD process. (b) Thermal resistance network.

Table 1
Common correlations used to estimate the heat transfer coefficient in membrane distillation. (From Phattaranawik et al. [2]).

Equation	Laminar or turbulent	Equation no.
$Nu = 1.86\left(\frac{RePr}{L/D}\right)^{1/3}$	L	L1
$Nu = 4.36 + \frac{0.036RePr(D/L)}{1+0.0011(RePr(D/L))^{0.8}}$	L	L2
$Nu_{cooling} = 11.5(RePr)^{0.23}(D/L)^{0.5}$ $Nu_{heating} = 15(RePr)^{0.23}(D/L)^{0.5}$	L	L3
$Nu = 0.13Re^{0.64}Pr^{0.38}$	L	L4
$Nu = 1.95\left(\frac{RePr}{L/D}\right)^{1/3}$	L	L5
$Nu = 0.097Re^{0.73}Pr^{0.13}$	L	L6
$Nu = 3.66 + \frac{0.104RePr(D/L)}{1+0.0106(RePr(D/L))^{0.8}}$	L	L7
$Nu = (1+\frac{6D}{L})\left(\frac{(f/8)RePr}{1.07+12.7(f/8)^{1/2}(Pr^{2/3}-1)}\right)$	T	T8
$Nu = (1+\frac{6D}{L})\left(\frac{(f/8)(Re-1000)Pr}{1+12.7(f/8)^{1/2}(Pr^{2/3}-1)}\right)$	T	T9
$Nu = 0.023(1+\frac{6D}{L})Re^{0.8}Pr^{1/3}$	T	T10
$Nu = 0.036Re^{0.8}Pr^{1/3}(\frac{D}{L})^{0.055}$	T	T11
$Nu = (1+\frac{6D}{L})\left(\frac{(f/8)RePr}{1.2+13.2(f/8)^{1/2}(Pr^{2/3}-1)}\right)$	T	T12
$Nu = 0.027(1+\frac{6D}{L})Re^{0.8}Pr^{1/3}\left(\frac{\mu_{bulk}}{\mu_{sur}}\right)^{0.14}$	T	T13

including those theoretical modeling or experimental work, adopts an approach by selecting certain correlations from the literatures. Some typical correlations being selected is tabulated in Table 1 which were summarized by Phattaranawik et al. [2]. The researchers then test the correlations against some experimental data either from their own measurement or from other literatures and claim the most suitable one of the selected correlations. This approach seems feasible but may actually mislead the readers about the "most suitable correlation" itself. For the correlations tabulated in Table 1, Eq. (L1) is regarded as the most used in the literatures (e.g., [3–5]). Martínez-Díez and Vázquez-González [3] found that various correlations may lead to significant departure between measurements and predictions, and Eq. (L1) is in satisfactory agreement with the experimental results. Banat et al. [4] found Eq. (L1) is applicable for laminar flow condition, and for turbulent flow condition the Dittus & Boleter type Eq. (T10) applies. Based on the heat and Mass analogy, Martínez-Díez and Vázquez-González [5] extends the applicability of Eq. (L1) to predict mass transfer subject to concentration polarization, and satisfactory agreement was reported. In addition, the heat transfer performance is related to the geometry and operation condition. For instance, natural convection (or mixed convection) may cast certain influences on the overall transport process. Kadir et al. [6] examined the heat transfer and friction correlations of a rectangular channel subject to finned surface. They found the heat transfer performance is depending on hydraulic diameter, the distance between fins in the flow direction and fin arrangement. Dogan and Sivrioglu [7] investigated mixed convection heat transfer from longitudinal fins inside a horizontal channel in the natural convection dominated region for a wide range of Rayleigh numbers and different fin heights and spacings. Their experimental results implicated study show that the dimensionless optimum fin spacing occurs for an aspect ratio between 0.08 and 0.12.

For laminar flow condition, as noted, geometry and boundary conditions can significantly affect the heat transfer correlation. For instance, for circular duct under fully thermally developed condition, the Nusselt number for constant temperature condition is 3.66 while it is 4.36 for constant heat flux condition. In typical MD operation, the boundary conditions are neither constant temperature nor constant heat flux. Meanwhile, influence of developing may prevail hydraulically, thermally, and simultaneously. These will certainly reinforce the uncertainty of selecting

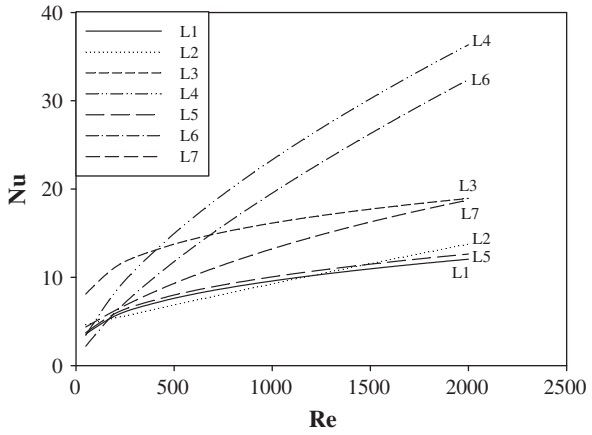

(a) Evaluations are performed at a feed temperature of 20 °C

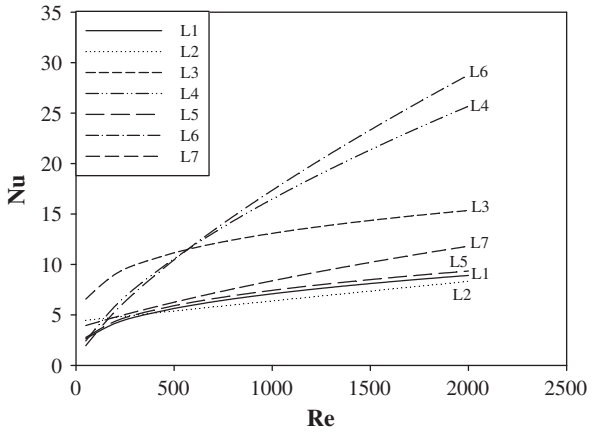

(b) Evaluations are performed at a feed temperature of 70 °C

Fig. 2. Variation of Nusselt number vs. Reynolds number subject to laminar flow condition. The Eqs. (L1…L7) are tabulated from Table 1. (a) Evaluations are performed at a feed temperature of 20 °C. (b) Evaluations are performed at a feed temperature of 70 °C.

correlations. For further comparison about the tabulated correlations, one can see the results in Fig. 2 showing the variation of heat transfer performance with the rise of the Reynolds number under laminar flow condition. As shown in the figure, significant differences of the predicted Nusselt number are encountered. For a Reynolds number around 2000, the calculation by Eq. (L4) is about 3.3 times higher than that of Eq. (L1) at a feed temperature of 70 °C, yet the difference increases to about 4 times at an even lower temperature of 20 °C as appeared in Fig. 2b. Note that the exponents of the Reynolds number for Eq. (L4) and Eq. (L6) are 0.64 and 0.73, respectively, which are unexpected high pertaining to laminar flow condition. Excluding the unexpected over-prediction by Eqs. (L4) and L6, the other correlation like Eq. (L3) is still about two times higher than that of Eq. (L1). The significant departure of the correlations may be associated with the real experimentation. For instance, the membrane is usually accompanied with some or with some supporting means which inevitably lead to a higher heat transfer performance. Contrast to that of laminar flow correlation, the correlations valid for turbulent flow shows only mild difference. As shown in Fig. 3, the maximum deviation is around 30–40%. In summary of the comparison, one can conclude a diversity amid the existing correlations particularly for laminar flow

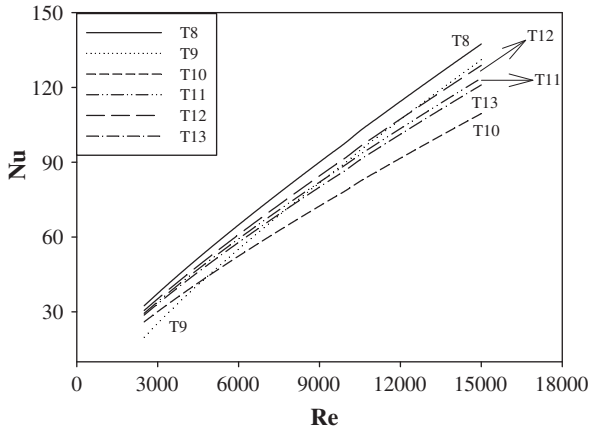

(a) Evaluations are performed at a feed temperature of 20 °C

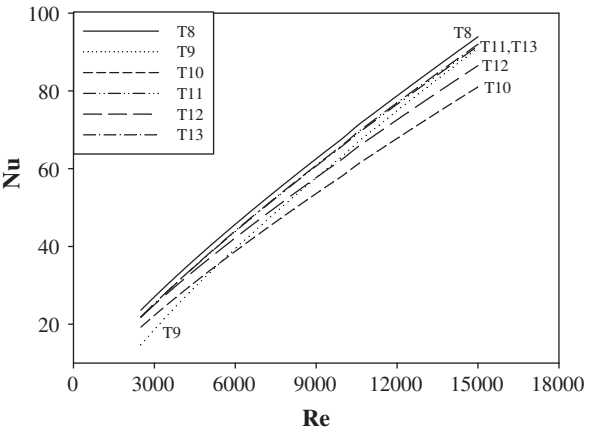

(b) Evaluations are performed at a feed temperature of 70 °C

Fig. 3. Variation of Nusselt number vs. Reynolds number subject to transition and turbulent flow condition. The Eqs (T8...T13) are tabulated from Table 1. (a) Evaluations are performed at a feed temperature of 20 °C. (b) Evaluations are performed at a feed temperature of 70 °C.

condition. And it should be stressed that most applications may be involved in laminar flow condition which make the correctness of the laminar flow correlation especially crucial.

Things get even more complicated as the flow passages are not in circular shape such as rectangular or plate channels. The imposed heating condition may just appear in the membrane side while other sides are either insulated or in contact with other channels. This eventually provides some uncertainties when applying existing correlations. However, the existing literatures still provides limited information about the selection or data reduction of this resistance. Therefore the objective of the present effort is to summarize and to recommend the correct way to obtain the feed side resistance in the subsequent discussion.

2. Data reduction of the thermal resistance at feed side and permeate side

Despite considerable experimental work being made during the past, as aforementioned, there is no heat transfer coefficient reported directly from the data reduction of measurements. Prior to discussing this unusual consequence, let's review the typical data reduction method in heat transfer experiments. Consider a typical counter flow arrangement without any mass transfer being taken place across the membrane as seen in Fig. 1a, the total heat transfer rate used in the calculation for the membrane module (or heat exchanger) is from the mathematical average of the feed side and permeate side, namely,

$$\dot{Q}_f = \dot{m}_f c_{p,f}(T_{f,in} - T_{f,out}) \tag{7}$$

$$\dot{Q}_p = \dot{m}_p c_{p,p}(T_{p,out} - T_{p,in}) \tag{8}$$

$$\dot{Q}_{ave} = (\dot{Q}_f + \dot{Q}_p)/2 \tag{9}$$

In a well-controlled experimental condition, the heat unbalance amid both sides should be less than 2% or 3%. From the rating equation for the overall heat transfer rate, one can obtain the overall resistance as:

$$\frac{1}{UA} = \frac{\Delta T_{LM}}{\dot{Q}_{ave}} \tag{10}$$

where ΔT_{LM} is the log mean temperature difference, designated as

$$\Delta T_{LM} = \frac{(T_{f,in} - T_{p,out}) - (T_{f,out} - T_{p,in})}{\ln\left(\frac{T_{f,in} - T_{p,out}}{T_{f,out} - T_{p,in}}\right)} \tag{11}$$

The overall resistance ($1/UA$) product is related to the individual resistance:

$$\frac{1}{UA} = \frac{1}{h_f A_f} + \frac{\delta}{k_m A_m} + \frac{1}{h_p A_p} \tag{12}$$

Consider a symmetrical flat membrane having the same surface area in both side, the foregoing equation can be simplified as:

$$\frac{1}{U} = \frac{1}{h_f} + \frac{\delta}{k_m} + \frac{1}{h_p} \tag{13}$$

In this regard, if one of the thermal resistance is known (e.g. $1/h_p$), the associated thermal resistance in the feed side can be obtained by subtracting the wall resistance and the permeate resistance from then overall resistance, i.e.,

$$\frac{1}{h_f} = \frac{1}{U} - \frac{\delta}{k_m} - \frac{1}{h_p} \tag{14}$$

Through this simple data reduction, the heat transfer coefficient can be easily estimated from Eq. (14). Regardless the process is quite straightforward and is easily implemented for typical experimentation; the success of this approach relies heavily on two important matters. The first one is the correctness of the correlation being used to back out in the permeate side. To resolve this issue, one usually intentionally places the permeate side in a more well-known and controlled conditions. For instance, the permeate side is placed in the tube side while the feed side is located at the shell side. With this arrangement, the permeate side heat transfer coefficient, h_p, is evaluated from the Dittus–Boelter type correlation or Gnielinski semi-empirical correlation with considerable accuracy. However, one should bear in mind that the Dittus–Boelter correlation is applicable in turbulent flow whereas the Gnielinski equation is valid provided Re > 2300. The second issue that affects this approach is even more vital, that are the magnitude of the thermal resistances of permeate side and wall surface. Apparently the overall thermal resistance $1/U$ is larger than individual resistances. To improve the accuracy of the calculated feed side resistance from Eq. (14), it is important to minimize the corresponding wall and permeate resistance. Smaller resistances will improve the accuracy of feed side resistance during subtraction. This is associated with the error propagation during subtraction. A larger thermal resistance results in larger uncertainty during subtraction, yet the uncertainty is further amplified when the individual resistance is above 50%. In

practice, it would be better to control the individual resistance to be less than 25%. Typical experimental techniques to minimize the thermal resistance of the permeate side are raising the fluid flow velocity or put augmentation such as inserts, roughness, or added surfaces at the permeate side.

3. Additional uncertainty caused by the membrane process

The data reduction method described in previous section is actually more appropriate for conventional heat exchanger. There are two additional uncertainties associated with the membrane process. The first one is the effect of mass transfer across the membrane that affects the heat transfer at feed side as well as permeate side. The effect of mass transfer on heat transfer is termed Ackemann correction factor, Qtaishat et al. [8] and Phattaranawik and Jiraratananon [9] had examined its influence on the overall heat transfer performance. The presence of mass transfer on the overall heat transfer rate is rather small. The analysis by Qtaishat et al. [8] showed that the effect of mass transfer increased with the rise of feed temperature, yet the effect in the feed side is larger than that of permeate side. The maximum increased values from mass transfer on the overall heat transfer is 4.3% and 1.43%, respectively at an average feed side temperature of 55.93 °C and a permeate side temperature of 18.28 °C. Analogously results were also reported by Phattaranawik and Jiraratananon [9]. A maximum influence of about 13% is encountered at a feed temperature of 368 K. The appreciable effect of 13% is related to the high feed temperature where the influence mass transfer is enormous as it approaches the boiling point. Normally this is unlikely to happen for a typical MD process. As a consequence, it can be concluded that the effect of mass transfer on heat transfer is small provided tests are conducted away from the saturation temperature.

The second uncertainty with the membrane is from the membrane itself. As seen from Eq. (14) where the feed side resistance is obtained by subtracting the membrane and permeated side resistance from the overall resistance. Again, the uncertainty rises considerably with the membrane resistance. Note that typical heat exchanger usually employ metals whose thermal conductivity can easily surpass tens or hundreds of W/m K, yielding a rather small wall resistance. However, typical thermal conductivity applicable to MD spans amid 0.04–0.06 W/m K which yields a quite percentage of the total resistance even for a very thin membrane. In fact, for a typical membrane thickness of 150 μm, a simple estimation reveals that the membrane resistance could easily surpass 50% or 60% at a lower feed temperature of 20 °C of the total resistance while the resistance is reduced to 20–30% when the feed temperature is raised over 70 °C. The results suggest a dramatic inaccuracy associated with direct subtraction approach for membranes, especially the data in low temperature. To increase the accuracy of the direct subtraction, the easiest way is simply to perform tests at a more elevated temperature but again it has the drawback of losing important data at lower temperature. Another way is to adopt the hybrid membrane. A more thin functionalized membrane layer is placed at the feed side and a support layer with large porosity is adhered to the thin layer to reduce the conduction loss.

4. Proposed data reduction procedure to obtain the heat transfer coefficient at feed side

Based on the forgoing discussion, it seems quite difficult to obtain the correct heat transfer coefficient from the experiments under membrane distillation process. The direct subtraction method has some inherited flaws, yet existing correlations may be inapplicable. To this regard, the present author proposes the Wilson plot method to obtain the heat transfer coefficient from the experimental data with a much higher accuracy. The method has been briefly cited for calculation of mass transfer coefficient (permeability, e.g. [10,11]) but is never fully addressed to achieve the heat transfer coefficient in membrane distillation. The subsequent outline is a modification to conventional Wilson plot method applicable to obtain the heat transfer coefficient. Through this approach, one can eliminate the uncertainty from permeate side and reduce the uncertainty in membrane to obtain a more reliable heat transfer coefficients at feed side from the experimentation.

1. Conduct experiments for membrane distillation, obtain the four terminal temperatures at the feed side and permeate side. Hence one can calculate the associate heat transfer rate and the logarithmic mean temperature difference, respectively:

$$Q = UA\Delta T_{LMTD} = \dot{m}c_{p,f}(T_{f,o} - T_{f,i}) \tag{15}$$

$$\Delta T = \frac{(T_{f,o} - T_{p,i}) - (T_{f,i} - T_{p,o})}{\ln\left(\frac{T_{f,o}-T_{p,i}}{T_{f,i}-T_{p,o}}\right)} \tag{16}$$

   Notice that it is suggested that the temperature difference in feed side or permeate side should be at least 2 °C as suggested for common heat exchanger test to minimize the measurement uncertainty (Wang et al. [12]).
2. The overall resistance can be easily estimated as:

$$R_t = \frac{1}{U} = \frac{1}{h_f} + \frac{1}{\frac{k_m}{\delta} + \frac{J\lambda}{\Delta T_m}} + \frac{1}{h_p} = R_f + R_m + R_p \tag{17}$$

3. Measure the flux, J, from the experiment.
4. To obtain the feed side resistance (heat transfer coefficient) via Wilson plot, it is a must to maintain a fixed permeate resistance throughout the test. This can be made possible by fixing an average permeate temperature and a fixed flow rate.
5. Unlike the convectional Wilson plot where the wall resistance (membrane resistance) stays unchanged, the membrane resistance is actually varying from experiment to experiment pertaining to flow conditions. Therefore, the membrane resistance must be subtracted from the overall resistance.
6. The heat transfer performance in feed side is generally assumed to be the following form:

$$Nu = C_0 \mathrm{Re}^a \mathrm{Pr}^b \tag{18}$$

   Note that an iteration process must be fulfilled before finally arrived at the correct exponent values of a and b. Initially, one can presume some values of a and b. As a consequence, the heat feed side transfer coefficient is obtained:

$$h_f = C_0\left(\frac{\rho_f v_f D}{\mu_f}\right)^a \left(\frac{\mu_f c_{p,f}}{k_f}\right)^b \frac{k_f}{D} = C_0 k_f^{1-b} \rho_f^a c_{p,f}^b \mu_f^{b-a} D^{a-1} v_f^a = C_1 v_f^a \tag{19}$$

7. Estimate the effective thermal conductivity,

$$k_m = (1-\varepsilon)k_s + \varepsilon k_g \tag{20}$$

   This term is rather insensitive to change of temperature and is independent of flow condition.
8. From the experimental measurement,

$$\dot{Q} = \dot{m}c_{p,f}(T_{f,o} - T_{f,i}) = \dot{Q}_m = \left(\frac{k_m}{\delta}\Delta T_m + J\lambda\right)A \tag{21}$$

   The temperature across membrane ΔT_m is then obtained.
9. Calculate the membrane resistance

$$R_m = \frac{1}{\frac{k_m}{\delta} + \frac{J\lambda}{\Delta T_m}} \tag{22}$$

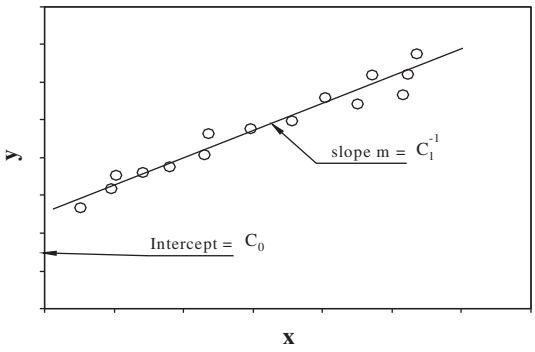

Fig. 4. Schematic of the Wilson plot technique to obtain the feed side heat transfer coefficients.

10. Rearranging the overall resistance equation in the following,

$$R_t = \frac{1}{U} = \frac{1}{C_1 v_f^a} + \frac{1}{\frac{k_m}{\delta} + \frac{J\lambda}{\Delta T_m}} + C_2 \tag{23}$$

The foregoing equation can thus be arranged to have the following form:

$$\frac{1}{U} - \frac{1}{\frac{k_m}{\delta} + \frac{J\lambda}{\Delta T_m}} = \frac{1}{C_1 v_f^a} + C_2 \tag{24}$$

The above equation takes the form as

$$y = mx + c \tag{25}$$

with

$$y = \frac{1}{U} - \frac{1}{\frac{k_m}{\delta} + \frac{J\lambda}{\Delta T_m}}$$

$$m = \frac{1}{C_1}$$

$$x = v_f^{-a}$$

$$c = C_2$$

11. By changing the velocity in the feed side, one can have a plot of y verse x on a linear scale as shown in Fig. 4. However, if the pot is not linear, one should adjust the corresponding values of *a* and *b* to achieve the linearity. The slope m and the intercept c are then determined from the plot. With *m*, the heat transfer coefficient in the feed side can be obtained.

5. Conclusion

The present study discusses the heat transfer coefficients applicable for membrane distillation. In the available literatures, most researchers adopt some existing correlations and test the applicability of these correlations to their test data or models. Unfortunately this approach is quite limited and extrapolation of this approach to other conditions is quite questionable. This is subject to the influences of boundary conditions, geometrical configurations, entry flow conditions, as well as some influences from spacer or support.

The simple way is to obtain the heat transfer coefficients from experimentation. However there is no direct experimental data for heat transfer coefficients being reported directly from the measurements. The reasons for this unusual situation are attributed to some causes mainly because it is very difficult to obtain heat transfer coefficients from direct subtraction of the individual resistances from the overall resistances. The main reasons are from the uncertainty of permeate side and the comparatively large magnitude of membrane resistance. Additional minor influence is the effect of mass transfer on the heat transfer performance. However, the mass transfer effect is negligible provided the feed side temperature is low. To increase the accuracy of the measured feed side heat transfer coefficient, it is proposed in this study to exploit a modified Wilson plot technique. Through this approach, one can eliminate the uncertainty from permeate side and reduce the uncertainty in membrane to obtain a more reliable heat transfer coefficient at feed side from the experimentation.

Acknowledgements

This work was supported by the Energy Bureau and Department of Industrial Technology, both from Ministry of Economic Affairs, Taiwan.

References

[1] Lawson KW, Lloyd DR. Membrane distillation. II direct contact MD. J Membrane Sci 1996;120:123–33.
[2] Phattaranawik J, Jiaratananon R, Fane AG. Heat transport and membrane distillation coefficients in direct contact membrane distillation. J Membrane Sci 2003;212:177–93.
[3] Martínez-Díez L, Vázquez-González MI. Temperature and concentration polarization in membrane distillation of aqueous salt solutions. J Membrane Sci 1999;156:265–73.
[4] Banat FA, Abu Al-Rub FA, Jumah R, Al-Shannag M. Modeling of desalination using tubular direct contact membrane distillation modules. Sep Sci Technol 1999;34:2191–206.
[5] Martínez-Díez L, Florido-Díaz FJ. Theoretical and experimental studies on desalination using membrane distillation. Desalination 2001;139:373–9.
[6] Bilen Kadir, Ugur A, Sinan Y. Heat transfer and friction correlations and thermal performance analysis for a finned surface. Energy Convers Manage 2001;42:1071–83.
[7] Dogan M, Sivrioglu M. Experimental investigation of mixed convection heat transfer from longitudinal fins in a horizontal rectangular channel: in natural convection dominated flow regimes. Energy Convers Manage 2009;50:2513–21.
[8] Qtaishat M, Matsuura T, Kruczek B, Khayet M. Heat and mass transfer analysis in direct contact membrane distillation. Desalination 2008;219:272–92.
[9] Phattaranawik J, Jiaratananon R. Direct contact membrane distillation: effect of mass transfer on heat transfer. J Membrane Sci 2001;188:137–43.
[10] Khayet M, Velázquez A, Mengual JI. Modelling mass transport through a porous partition: effect of pore size distribution. J Non-Equilib Thermodyn 2004;29:279–99.
[11] Drioli E, Criscuoli A, Curcio E. Membrane contactors: fundamentals, applications and potentialities. Elsevier press; 2006 [chapter 5, p. 181].
[12] Wang CC, Webb RL, Chi KU. Data reduction of air-side performance of fin-and-tube heat exchangers. Exp Therm Fluid Sci 2000;21:218–26.